Evaluation of Quantitative 68Ga-PSMA PET/CT Repeatability of Recurrent Prostate Cancer Lesions Using Both Standard and Bayesian Penalized Likelihood Reconstruction Algorithms

Mark J Roef (mark.roef@catharinaziekenhuis.nl)
Catharina Ziekenhuis https://orcid.org/0000-0002-1772-8474
Sjoerd Rijnsdorp
Ziekenhuis Amstelland
Christel Brouwer
Catharina Ziekenhuis
Dirk Wyndaele
Catharina Ziekenhuis
Albert J. Arends
Catharina Ziekenhuis

Original research

Keywords: Repeatability, 68Ga-PSMA PET/CT, Bayesian penalized likelihood reconstruction

Posted Date: September 10th, 2020

DOI: https://doi.org/10.21203/rs.3.rs-68827/v1

Abstract

Purpose To formally determine the repeatability of ^{68}Ga-PSMA lesion uptake in both relapsing and metastatic tumour. In addition, it was hypothesized that the Bayesian penalized likelihood algorithm Q.Clear has the ability to lower SUV signal variability in the small lesions typically encountered in PET images of early relapse or early metastatic disease of prostate cancer.

Methods Patients with biochemical recurrence of prostate cancer were prospectively enrolled in this pilot test-retest study and underwent two ^{68}Ga-PSMA PET/CT scans within on average 7.9 days. Lesions were classified by two independent readers as suspected local recurrence, lymph node metastases or bone metastases. Two datasets were generated: one standard ordered subset expectation maximization (OSEM) reconstruction incorporating both time-of-flight (TOF) and point spread function (PSF) modelling, and one with the Bayesian penalized likelihood (BPL) reconstruction algorithm, called Q.Clear. For tumour lesions the maximum standardized uptake value (SUVmax) were determined. Repeatability was formally assessed using Bland-Altman analysis for both BPL and standard reconstruction.

Results A total number of 65 PSMA-positive tumour lesions were found in 23 patients (range 1 to 12 lesions a patient). Another 7 patients had no detectable lesions and were therefore excluded. Overall repeatability in the 65 lesions was -1.5% ± 22.7% (SD) on standard reconstructions and -2.1% ± 29.1% (SD) on BPL reconstructions. The difference was not statistically significant. ^{68}Ga-PSMA SUVmax had upper and lower limits of agreement of +42.9% and -45.9% for standard reconstructions and +55.0% and -59.1% for BPL reconstructions, respectively. Tumour SUVmax repeatability was dependent on lesion area, with smaller lesions exhibiting poorer repeatability on both standard and BPL reconstructions (F-test, $p < 0.0001$).

Conclusion ^{68}Ga-PSMA SUVmax has relatively high upper and lower limits of agreement for both standard and BPL reconstructions in the small lesions typical for early relapse or early metastatic disease of prostate cancer. BPL does not seem to lower signal variability in these cases.

Introduction

In western Europe, United States and Canada prostate cancer has the highest incidence of all cancers in men, with a global incidence estimated at over 1.6 million in 2015 (1) Although many prostate cancers have a relatively indolent behaviour and do not lead to significant problems during the lifetime of a patient, patients may eventually progress to metastatic and/or castration resistant prostate cancer (CRPC), which is considered an incurable and fatal stage of the disease (2,3).

The optimal treatment for metastatic prostate cancer depends on characteristics of the tumour and of the patient, and may consist of multiple modalities including hormone, chemo, external beam radiation, and radionuclide therapy (4). The effectiveness of any treatment should be monitored, in order to refrain from ineffective therapy, unneeded costs and avoidable side effects.

The response to treatments for prostate cancer is generally evaluated using PSA measurements. However, PSA provides a very limited correlation with histopathological response and survival, and merely reflects an approximation of the average response in all lesions (5). Specific tumour lesions may vary in response, and selective treatments are increasingly applied for individual clinically relevant lesions (6) or selected types of metastases such as bone metastases (7). Therefore, monitoring of lesion-specific response to treatment is becoming more relevant, but cannot be provided using PSA measurements. In addition, anatomical imaging modalities such as CT and MR are considered unreliable for evaluation of response in bone lesions (8) and skeletal scintigraphy is unable to discriminate response and signal flare due to bone repair (9). Metabolic imaging with ^{18}F-FDG PET has limited sensitivity for prostate cancer and is potentially

compromised by inflammation after irradiation. (10). There is need for a tool that provides quantitative, lesion-specific and observer-independent response evaluation, regardless of their location.

Functional metabolic imaging with ^{68}Ga-PSMA and positron emission tomography (PSMA-PET) is potentially such a tool because PSMA is expressed irrespective of PSA levels or tumour proliferation rate and can be targeted in PSMA directed radionuclide therapy (11,12). However, a standardized quantitative approach still needs to be developed.

It is known that uptake measurements of radiolabeled tracers with PET in vivo suffer from many inaccuracies, as demonstrated by experience with FDG (13), and that this requires evaluation and standardisation prior to application as response parameter (14). This probably applies equally to PSMA-PET expression. Before quantification of PSMA expression can be used as a biological parameter to identify response to treatment, and before we can design sufficiently powered response evaluation studies, we need to know the characteristics of the measurement technique. An important factor that is currently less known is the normal day-to-day variability in ^{68}Ga-PSMA expression of tumour, i.e. repeatability.

The main aim of this pilot study is to formally determine the repeatability of ^{68}Ga-PSMA in both relapsing and metastatic tumour. First presentation of tumour relapse or metastatic disease in prostate cancer often is limited in nature both in number and size. The latter causes partial volume effects (PVEs) to become increasingly relevant. Partial volume effects start to play a role when lesion size falls below 2 to 3 times the resolution of the PET system, i.e. below 10 to 15 mm for an average PET/CT scanner system (15), and are expected to increase signal variability. Several strategies have been described that attempt to correct for these partial volume effects, both post reconstruction and during reconstruction of the images (16,17).

The Bayesian penalized likelihood (BPL) reconstruction algorithm called Q.Clear (GE Healthcare, Milwaukee, USA) is such an algorithm that is correcting for partial volume effects during image reconstruction, resulting in higher uptake/expression values compared to standard reconstruction (16). We hypothesize that Q.Clear has the ability to lower signal variability in the small lesions typically encountered in early relapse or early metastatic disease of prostate cancer, the **second aim** of the study.

Materials And Methods

Patients

Thirty patients with biochemical recurrence of prostate cancer scheduled for routine clinical ^{68}Ga-PSMA PET/CT were prospectively enrolled in this pilot study (NL52809.100.16/R16.058/Ga68-PSMA test-retest study) between January 2018 and July 2019. Their scans were screened for evaluable PSMA-positive tumor lesions by two board certified nuclear physicians (MJR and CB). Seven patients had no evaluable tumor lesions and were excluded from the study. The remaining twenty-three had their second (retest) scan within on average 7.9 days of their initial (test) scan and were evaluated for measurements in assigned tumour lesions. Tumour lesions were classified as suspected local recurrence, lymph node metastases or bone metastases. Both baseline scans were performed before any treatment had begun. The study was approved by the local institutional ethics review board and all patients had given written approval before any scan was done.

PET images were acquired on a PET/CT scanner (GE Healthcare Discovery 710), with a 2.5 min acquisition per bed position, on average 58 (range 55 to 69) min after injection of on average 1.4 (range 0.9 to 1.7) MBq/kg dose of ^{68}Ga-PSMA. Two datasets were reconstructed: one standard ordered subset expectation maximization (OSEM) reconstruction including both time-of-flight (TOF) and point spread function (PSF) modelling, and a second one using the Bayesian penalized likelihood (BPL) algorithm, called Q.Clear (18). Both used low dose CT for attenuation correction. For the BPL

algorithm, a beta value of 600 was used. This value was found optimal in a ^{68}Ga-PSMA phantom study using spheres of 5-37 mm diameter (unpublished results).

PET and CT analysis

For both the test and the retest datasets, the PET and low-dose CT images were processed independently. Imaging reading was performed using dedicated software for PET/CT imaging (Philips intellispacePortal).

In PET, tumour lesion size was measured in the axial plane using a fixed PET windowing upper level (UL) of 10 used for stretching of the greyscale. Both long and short axis were measured, lesion area was calculated according to the simple formula for round and oval lesions: A= π x half long axis x half short axis. Within this area the pixel with the highest standardized uptake value is designated the SUVmax (injected dose/kg body weight). Thus SUVmax was measured in all tumour lesions. The small size of most of the lesions did not allow for measurement of other meaningful SUVs such as SUVpeak that need lesions of at least 1 cm^3. Low dose CT was used to check for appropriateness of the lesion area measured in PET if possible (i.e. with the exception of some bone metastases not visible on CT).

Statistical analysis

The repeatability of SUVmax in tumour lesions was assessed with Bland-Altman analysis by reporting the mean (bias) and limits of agreement (defined as mean±1.96 SD) of the differences between the two measurements of individual lesions. Bland-Altman analysis was preferred over intra class correlation coefficients on the basis of previous recommendations (19,20). Assessment of signal variability between lesion areas and SUVmax was assessed with F-testing.

For the comparison of the two reconstruction techniques a paired t-test was used, i.e. BPL versus standard.

Results

A total number of 65 PSMA-positive tumour lesions were found in 23 patients (range 1 to 12 lesions), see table 1 for patient characteristics. In addition, in 7 patients no lesions were found, and therefore these were excluded. In theory, a perfect test-retest will result in identical values for the test and the retest. In daily practice however, measurements of a lesions SUVmax in repeated acquisitions will yield results normally distributed around the true value. In tumour lesions showing an increased SUVmax from test to retest the average increase was 16.8% ± 10.6% (SD) on standard reconstructions (33 lesions) and 22.1% ± 18.6% (SD) on BPL reconstructions (30 lesions). In tumour lesions showing a decreased SUVmax from test to retest these values were -21.0% ± 15.2% (SD) on standard reconstructions (32 lesions) and -23.2% ± 19.7% (SD) on BPL reconstructions (35 lesions), respectively. Overall repeatability in 65 lesions was -1.5% ± 22.7% (SD) on standard reconstructions and -2.1% ± 29.1% (SD) on BPL reconstructions. The small difference between both reconstructions was not statistically significant.

Figure 1 displays the repeatability results of SUVmax for both reconstructions in all lesions (65 lesions, Figure 1A), local recurrences (9 lesions, Figure 1B), lymph node metastases (36 lesions, Figure 1C) and bone metastases (20 lesions, Figure 1D).

As shown in Figure 1A overall repeatability of SUVmax had upper and lower limits of agreement of +42.9% and -45.9% for standard reconstructions and +55.0% and -59.1% for BPL reconstructions, respectively. For suspected local recurrence SUVmax had a repeatability of -5.0% ± 14.4%, with upper and lower limits of agreement of +23,2% and -33,1% for standard reconstructions. For BPL reconstructions SUVmax repeatability was -9.5% ± 16.8%, with upper and lower limits at +23.5% and -42.5%. See Figure 1B. For suspected lymph node metastases SUVmax repeatability was -4.5% ± 22.8% for standard reconstructions, with upper and lower limits of +40.1% and -49.1%. For BPL reconstructions SUVmax

repeatability was -3.3% ± 30.6%, with upper and lower limits at +56.6% and -63,2%. See Figure 1C. For suspected bone metastases SUVmax had a repeatability of +4.4% ± 26.1%, with upper and lower limits of agreement of +55.7% and -46.8% for standard reconstructions. For BPL reconstructions SUVmax repeatability was +2.7% ± 32.8%, with upper and lower limits at +67.0% and -61.6%. See Figure 1D. None of the differences between standard and BPL reconstructions were statistically significant.

Tumour SUVmax repeatability was dependent on lesion area, with smaller lesions exhibiting poorer repeatability on both standard and BPL reconstructions (F-test, $p < 0.0001$). See Figure 2A and B.

Tumour absolute SUVmax was higher in BPL reconstructions than in standard reconstructions for all lesions (data not shown). The relative increase in measured SUVmax in the BPL reconstructions (as compared to standard reconstruction) was dependent on lesion size. Smaller lesions (lesion area < 200 mm^2) showed a significant larger increase of SUVmax as compared to larger lesions (lesion area > 200 mm^2): 44,3% ± 4,6% versus 25,5% ± 42,2% for the test scans ($p = 0,004$) and 43,5% ± 3,9% versus 18,6% ± 3,1% for the retest scans ($p < 0,001$), respectively. See table 2.

Discussion

In this prospective test-retest study we formally report the repeatability of ^{68}Ga-PSMA in both relapsing and metastatic tumour. The main finding of this study is the relatively high day-to-day variability of tumour SUVmax with repeatability levels of agreement varying between +43% and -46% for all lesions taken together. For local recurrences values vary between +23% and -33%, for the smaller lymph node and bone metastases values are +40% to -49% and +56% to -47%, respectively. In addition to this, we show a significant correlation between lesion size and SUVmax repeatability levels of agreement.

With respect to our second aim no significant differences in repeatability between standard (OSEM+TOF+PSF) reconstruction and (TOF+PSF) + BPL reconstruction could be shown in this pilot study. There was a small difference in favour of the standard reconstruction. However, BPL reconstructions resulted in significantly higher SUVmax of tumour lesions as compared to standard reconstructions, with significantly higher relative increases in smaller lesions.

Pollard et al. reported on the repeatability of ^{68}Ga-PSMA-HBED-CC (PSMA-11) SUVmax in relapsing prostate cancer (21). Repeatability levels of agreement were given for lymph node and bone metastases only and were lower than in our study: 30-40% versus 40-60%. Also for other radiotracers like ^{18}F-DCFPyL, ^{18}F-FDG and ^{18}F-FLT values in the 30-40% range were reported for SUVmax (22,23). A possible explanation for the higher day-to-day variability in our study is the relative high number of small lesions. Our study hints at a negative correlation between lesion SUVmax variability and lesion size (Figure 2A). We believe the patient cohort of this pilot study to be representative for patients with relapsing prostate cancer showing relatively small tumour lesions in lymph nodes and bones. Pollard et al. did not find any relationship between lesion size and SUVmax variability (21). A possible explanation for this is that they only reported on relationships within classes, i.e. within typically smaller lymph node and bone metastases, where we report on all lesions including the larger relapses of the primary tumour in the prostate bed.

A larger day-to-day variability may have implications for lesion-specific response to treatment monitoring. With respect to treatment response monitoring using ^{18}F-FDG Wahl et al. proposed a minimum of 30% SUVmax decrease for a true response in their PERCIST response criteria (24). A minimum of 30% response is probably not appropriate for the majority of the relatively small lesions that are typically found in (early) relapsing prostate cancer. Our study shows that a minimum response of 50% might be more appropriate in these cases, when using ^{68}Ga-PSMA.

Measurements of SUVmax are known to be considerably subject to noise and thus to higher signal variability (25). In order to overcome the drawback of noisy SUVmax, SUVpeak was proposed using a 1 cm^3 volume centered around the

voxel with the highest SUV (i.e. SUVmax) thus being less subject to noise. Unfortunately SUVpeak seems to be appropriate for larger tumour volumes only, because a 1 cm^3 volume would correspond to a sphere of at least 12 mm diameter. Most of the lymph node and bone metastases in our study had dimensions smaller than that. Thus SUVpeak was not used in our study. In addition, SUVmax is the SUV measurement that is widely used in the clinic.

When confronted with the relatively small tumour lesions in patients with (early) relapsing prostate cancer, partial volume effects have to be anticipated. This will be particularly the case when quantifying tracer expression in small lesions using tracers with high tumour-to-background ratios like ^{68}Ga-PSMA, but is not always appreciated (26,27). For example, in a report on the effects of androgen deprivation therapy on ^{68}Ga-PSMA SUVmax in primary prostate cancer, lymph node and bone metastases as recent as April 2020, possible impact of partial volume effects was not discussed at all (28).

The possible importance of partial volume effects can be illustrated by the BPL versus standard reconstructions, as applied in our study. Two factors that contribute to the partial volume effect (spill-in and spill-out) are the finite spatial resolution of the imaging system and image sampling on a voxel grid not exactly matching the actual contours of tracer distribution (17). Impact of partial volume effects is strongly dependent on lesion size and is coming into play when lesion size falls below 2 to 3 times the resolution of the system, i.e. below 10 to 15 mm for an average PET/CT scanner system (16). With respect to tracer SUVmax measurements, partial volume effect will generally result in lower SUVmax values. Correcting for the aforementioned factors (i.e. partial volume correction) is complex and not all factors can be controlled for from one imaging session to another, introducing possible biases. In addition, partial volume correction can be applied after image reconstruction but also during image reconstruction (18). The Bayesian penalized likelihood (BPL) reconstruction algorithm called Q.Clear can be regarded as an algorithm correcting for partial volume, because it has a component that is correcting at the voxel level during image reconstruction (16). The resulting higher uptake/expression values in small lesions (compared to standard reconstruction) have been reported for several radiotracers, including ^{18}F-PSMA-1007 in prostate cancer patients (29). In the latter study SUVmax with BPL reconstruction has been compared to standard (OSEM+TOF+PSF) reconstruction, stratified for lesion size. A significant reported increase in SUVmax with BPL reconstruction for lesions smaller than 10 mm diameter only was reported. In our study we confirm these findings for the ^{68}Ga-PSMA tracer, including the relationship with lesion size (table 1), thus highlighting the importance of partial volume effects and its correction.

We hypothesized that the BPL reconstruction algorithm Q.Clear has the ability to lower signal variability in the small lesions typically encountered in early relapse or early metastatic disease of prostate cancer. Our study did not confirm our hypothesis. In contrary, signal variability tended to be higher with BPL reconstruction compared to standard reconstruction. We speculate that the partial volume correction component of BPL reconstruction might be responsible for the higher signal variability. A possible explanation for this could be the ‘overshoot’ reported with BPL reconstruction for small spheres at high sphere-to-background ratios in a phantom study using ^{18}F-FDG (30). The high sphere-to-background ratios in this study may correspond to the high tumour-to-background ratios typically encountered in ^{68}Ga-PSMA avid prostate cancer lesions.

Limitations. This single site study has several limitations. The assignment of tumour lesions was only done by two experienced image readers, and inter-observer variability was not assessed. This was considered acceptable because the exact nature of the lesions was less important in light of the general aim of the study, i.e. assessment of signal variability. The same holds for the fact that for the majority of the lesions there has been no confirmation by histopathology.

With respect to the comparison of the BPL and standard reconstructions, the image reading was not blinded. This was deemed acceptable because the visual appearance of both reconstructions is different, precluding true blinded image reading.

No significant difference was found between BPL and standard reconstruction signal variability, probably because the study was underpowered. Being a pilot study, the results can be used for power calculations for a possible future study.

Conclusion

The main finding of this study is the relatively high day-to-day variability of tumour SUVmax with repeatability levels of agreement varying between +43% and -46% for all lesions taken together. Small lesions tend to have larger day-to-day variability of tumour SUVmax when compared to larger lesions. With respect to response monitoring, minimum response of 50% for ^{68}Ga-PSMA PET might be more appropriate.

With respect to our second aim no significant differences in repeatability between standard (OSEM+TOF+PSF) reconstruction and (TOF+PSF)+BPL reconstruction could be shown in this pilot study. There was a small difference in favour of the standard reconstruction, however.

Abbreviations

BPL: Bayesian penalized likelihood

^{18}F-DCFPyL: 18-Fluor(2-(3-{1-carboxy-5-[(6-^{18}F-fluoro-pyridine-3-carbonyl)-amino]-pentyl}-ureido)-pentanedioic acid)

^{18}F-FDG: 18-Fluor fluorodeoxyglucose

^{18}F-FLT: 18-Fluor fluoro-3'-deoxy-3'-L: -fluorothymidine

^{68}Ga-PSMA PET/CT: 68-Gallium prostate specific membrane antigen positron emission tomography/computed tomography

OSEM: Ordered subset expectation maximization

PSA: Prostate specific antigen

PSF: Point spread function

PSMA: Prostate specific membrane antigen

SUVmax: Maximum standardized uptake value

SUVpeak: Peak standardized uptake value

TOF: Time-of-flight

Declarations

Ethics approval and consent to participate The study was conducted in accordance with the Helsinki declarations. All patients signed an informed written consent form. The study protocol was approved by our regional ethics committee (MEC-U, approval on NL52809.100.16, R16.058/Ga68-PSMA test-retest study).

Consent for publication not applicable

Availability of data and material The datasets used and/or analysed during the current study are available from the corresponding author on reasonable request.

Competing interests The authors declare that they have no competing interests.

Funding The study was funded by General Electrics Health Care (investigator-sponsored research support for principal investigator Mark J. Roef). The study was investigator driven. General Electrics Health Care played no role in study design, data analysis or in writing the manuscript.

Authors' contributions MR was the leading contributor to study design, data analysis and interpretation as well as to writing the manuscript. SR and AA were major contributors to study design and to writing the manuscript. CB and DW were major contributors to data analysis and interpretation. All authors read and approved the final manuscript.

Acknowledgements First, we thank all the patients who agreed to participate in the study. Furthermore, we want to thank our PET/CT team for their excellent support. We would also like to thank Marcel van 't Veer for his statistical help.

References

1. Global Burden of Disease Cancer Collaboration. Global, Regional, and National Cancer Incidence, Mortality, Years of Life Lost, Years Lived With Disability, and Disability-Adjusted Life-years for 32 Cancer Groups, 1990 to 2015A Systematic Analysis for the Global Burden of Disease Study. JAMA Oncol. 2017;3:524–48.
2. van der Kwast TH, Roobol MJ. Defining the threshold for significant versus insignificant prostate cancer. Nat Rev Urol. 2013;10:473-82.
3. Attard G, Parker C, Eeles RA, Schröder F, Tomlins SA, Tannock I, et al. Prostate cancer. Lancet 2016;387:70-82.
4. Heidenreich A, Bastian PJ, Bellmunt J, Bolla M, Joniau S, van der Kwast T, et al. EAU guidelines on prostate cancer. Part II: Treatment of advanced, relapsing, and castration-resistant prostate cancer. Eur Urol. 2014;65:467-79.
5. Francini E, Petrioli R, Rossi G, Laera L, Roviello G. PSA response rate as a surrogate marker for median overall survival in docetaxel-based first-line treatments for patients with metastatic castration-resistant prostate cancer: an analysis of 22 trials. Tumour Biol. 2014;35:10601-7.
6. Khullar K, Parikh RR. The role of radiotherapy in metastatic prostate cancer. Am J Clin Exp Urol. 2019;7:92-97.
7. Kratochwil C, Haberkorn U, Giesel FL. Radionuclide Therapy of Metastatic Prostate Cancer. Semin Nucl Med. 2019;49:313-25.
8. Eisenhauer EA, Therasse P, Bogaerts J, Schwartz LH, Sargent D, Ford R, et al. New response evaluation criteria in solid tumours: revised RECIST guideline (version 1.1). Eur J Cancer. 2009;45:228-47.
9. Pollen JJ, Witztum KF, Ashburn WL. The flare phenomenon on radionuclide bone scan in metastatic prostate cancer. AJR Am J Roentgenol. 1984;142:773-6.
10. Jadvar H. Imaging evaluation of prostate cancer with 18F-fluorodeoxyglucose PET/CT: utility and limitations. Eur J Nucl Med Mol Imaging 2013; 40 Suppl 1: S5-10.
11. Afshar-Oromieh A, Avtzi E, Giesel FL, Holland-Letz T, Linhart HG, Eder M, et al. The diagnostic value of PET/CT imaging with the 68Ga-labelled PSMA ligand HBED-CCin the diagnosis of recurrent prostate cancer. Eur J Nucl Med Mol Imaging 2015; 42: 197-209.
12. Wester HJ, Schottelius M. PSMA-Targeted Radiopharmaceuticals for Imaging and Therapy. Semin Nucl Med. 2019;49:302-12.
13. de Langen AJ, Vincent A, Velasquez LM, van Tinteren H, Boellaard R, Shankar LK, et al. Repeatability of 18F-FDG uptake measurements in tumors: a metaanalysis. J Nucl Med. 2012;53:701-8.
14. Aide N, Lasnon C, Veit-Haibach P, Sera T, Sattler B, Boellaard R. EANM/EARL harmonization strategies in PET quantification: from daily practice to multicentre oncological studies. Eur J Nucl Med Mol Imaging. 2017;44(Suppl 1):17-31.

15. Bettinardi V, Castiglioni I, De Benardi E, Gilardi MC. PET quantification: strategies for partial volume correction. Clin Transl Imaging 2014;2:199-218.
16. Rousset O, Rahmim A, Alavi A, Zaidi H. Partial volume correction strategies in PET. PET Clin 2007;2:235-49.
17. Soret M, Bacharach SL, Buyat I. Partial-volume effect in PET tumor imaging. J Nucl Med. 2007;48:932-45.
18. Te Riet J, Rijnsdorp S, Roef MJ, Arends AJ. Evaluation of a Bayesian penalized likelihood reconstruction algorithm for low-counts clinical ^{18}F-FDG PET/CT. EJNMMI Physics 2019;6:32.
19. Zaki R, Bulgiba A, Ismail R, Ismail NA. Statistical methods used to test for agreement of medical instruments measuring continuous variables in method comparison studies: a systematic review. PLoS One 2012;7:e37908.
20. Lodge MA.Repeatability of SUV in Oncologic 18 F-FDG PET. J Nucl Med. 2017;58:523-32.
21. Pollard JH, Raman C, Zakharia Y, Tracy CR, Nepple KG, Ginader T, et al. Quantitative test-retest measurement of ^{68}Ga-PSMA-HBED-CC (PSMA-11) in tumor and normal tissue. J Nucl Med. 2019 Dec 5;jnumed.119.236083. doi: 10.2967/jnumed.119.236083. Online ahead of print
22. Jansen BHE, Cysouw MCF, Vis AN, van Moorselaar RJA, Voortman J, Bodar YJL, et al. Repeatability of Quantitative ^{18} F-DCFPyL PET/CT Measurements in Metastatic Prostate Cancer. J Nucl Med. 2020 Jan 10:jnumed.119.236075. doi: 10.2967/jnumed.119.236075. Online ahead of print.J Nucl Med. 2020
23. Hatt M, Cheze-Le Rest C, Aboagye EO, Kenny LM, Rosso L, Turkheimer FE, Albarghach NM, Metges JP, Pradier O, Visvikis D. Reproducibility of 18F-FDG and 3'-deoxy-3'-18F-fluorothymidine PET Tumor Volume Measurements. J Nucl Med. 2010;51:1368-76.
24. Wahl RL, Jacene H, Kasamon Y, Lodge MA. From RECIST to PERCIST: Evolving Considerations for PET Response Criteria in Solid Tumors. J Nucl Med. 2009;50 Suppl 1(Suppl 1):122S-50S.
25. Lodge MA, Chaudry MA, Wahl RL. Noise considerations for PET quantification using maximum an peak standardized uptake value. J Nucl Med 2012; 53:1041-7.
26. Afshar-Oromieh, A. Malcher, M. Eder et al., PET imaging with a [^{68}Ga]gallium-labelled PSMA ligand for the diagnosis of prostate cancer: biodistribution in humans and first evaluation of tumour lesions. Eur J Nucl Med Mol Imaging 2013;40:486-95.
27. Berliner, M. Tienken, T. Frenzel et al., Detection rate of PET/CT in patients with biochemical relapse of prostate cancer using [^{68}Ga]PSMA I&T and comparison with published data of [^{68}Ga]PSMA HBED-CC. Eur J Nucl Med Mol Imaging 2017;44:670-77.
28. Ettala O, Malaspina S, Tuokkola T, Luoto P, Löyttyniemi E, Boström PJ, et al. Prospective Study on the Effect of Short-Term Androgen Deprivation Therapy on PSMA Uptake Evaluated With ^{68} Ga-PSMA-11 PET/MRI in Men With treatment-naïve Prostate Cancer. EJNMMI 2020; 47: 665-73.
29. Witkowska-Patena E, Budzyńska A, Giżewska A, Dziuk M, Walęcka-Mazur A. Ordered Subset Expectation Maximisation vs Bayesian Penalised Likelihood Reconstruction Algorithm in 18F-PSMA-1007 PET/CT. Ann Nucl Med. 2020;34:192-99.
30. Yamaguchi S, Wagatsuma K, Miwa K, Ishii K, Inoue K, Fukushi M. Bayesian Penalized-Likelihood Reconstruction Algorithm Suppresses Edge Artifacts in PET Reconstruction Based on Point-Spread-Function. Phys Med. 2018 Mar;47:73-9.

Tables

Table 1. Patient characteristics

	Age	PSA	Gleason score at diagnosis	Total number of lesions	Prostate bed	Lymph node metastases	Bone metastases	Initial therapy	Year of therapy
Patient no.									
1	83	2.4	7	3	-	3	-	LND+EBRT	2009
2	71	4.1	8	1	-	-	1	RALP+LND	2017
3	75	4.5	7	1	-	-	1	RALP	2009
4	73	8.4	6	6	-	3	3	AS+BT+LND	2012-2016
5	69	0.7	7	2	-	2	-	RALP+ELND	2015
6	78	16.0	6	3	1	2	-	BT	2011
7	84	9.0	6	4	1	3	-	BT	2012
8	80	0.7	8	2	1	-	1	RALP+LND	2008
9	62	3.9	6	1	1	-	-	BT	2013
10	77	3.0	7	1	-	1	-	RALP+ELND	2010
11	71	3.5	7	1	1	-	-	BT	2014
12	67	5.7	-	3	1	1	1	BT	2007
13	78	1.7	8	1	-	1	-	BT	2016
14	75	2.8	6	3	-	3	-	BT	2009
15	74	2.0	7	1	-	1	-	RP+LND+EBRT	2009
16	77	1.2	7	3	-	3	-	RALP	2009
17	72	2.5	7	12	-	-	12	RALP+ELND	2018
18	73	2.8	7	1	-	-	1	BT	2007
19	78	5.4	6	3	-	3	-	RALP+LND	2008
20	77	3.7	8	4	2	2	-	EBRT+HT	2009
21	69	5.2	6	1	1	-	-	EBRT	2012
22	68	0.6	7	3	-	3	-	RALP+LND	2015
23	78	7.0	7	5	-	5	-	EBRT	2017

AS = active surveillance, BT = brachytherapy, EBRT = external beam radiotherapy, ELND = extended lymph node dissection, HT = hormonal therapy, LND = lymph node dissection, RP = radical prostatectomy (open procedure), RALP = robot assisted radical prostatectomy

Table 2. BPL SUVmax increase (relative to standard reconstruction) for smaller and larger lesions

	Test BPL relative increase of SUVmax (%)	SEM	Retest BPL Relative increase of SUVmax (%)	SEM
lesions < 200 mm2	44.3	4.6	43.5	3.9
lesions >= 200 mm2	25.5	4.2	18.6	3.1
2-sided t-test	P = 0.004		P < 0.001	

Figures

Figure 1A

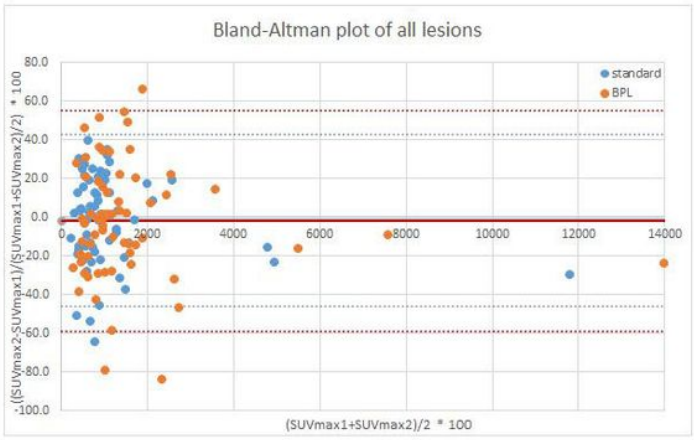

Figure 1C

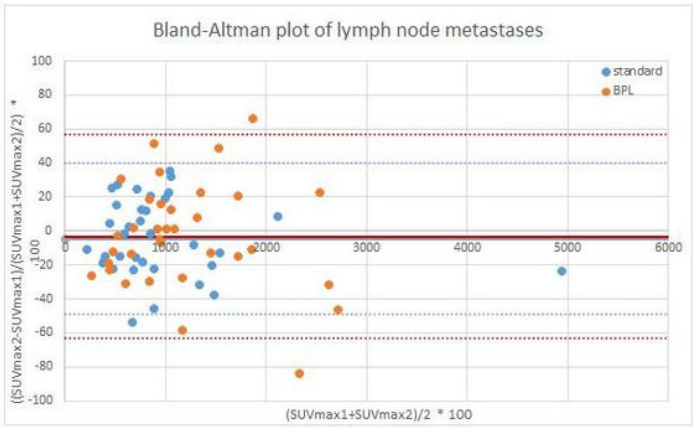

Figure 1B

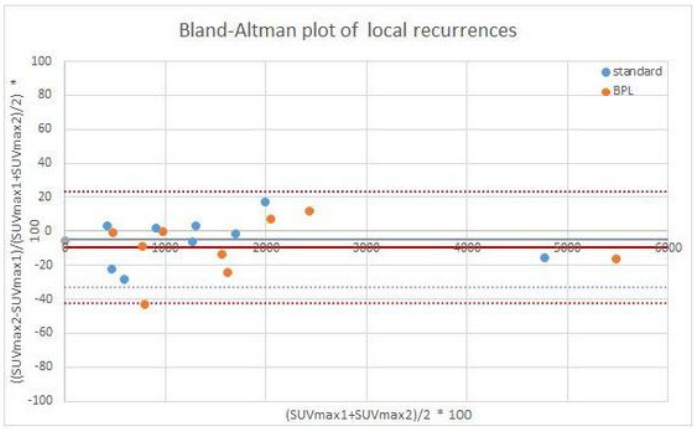

Figure 1D

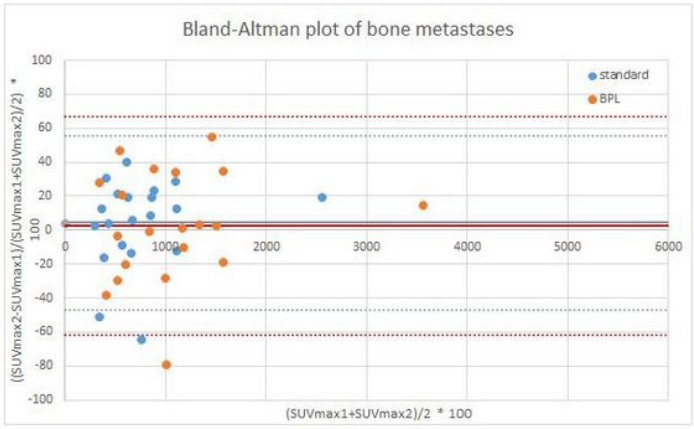

Figure 1

Bland-Altman plots of all lesions (1A), local recurrences (1B), lymph node metastases (1C) and bone metastases (1D), both for standard and BPL reconstructions.

Figure 2B

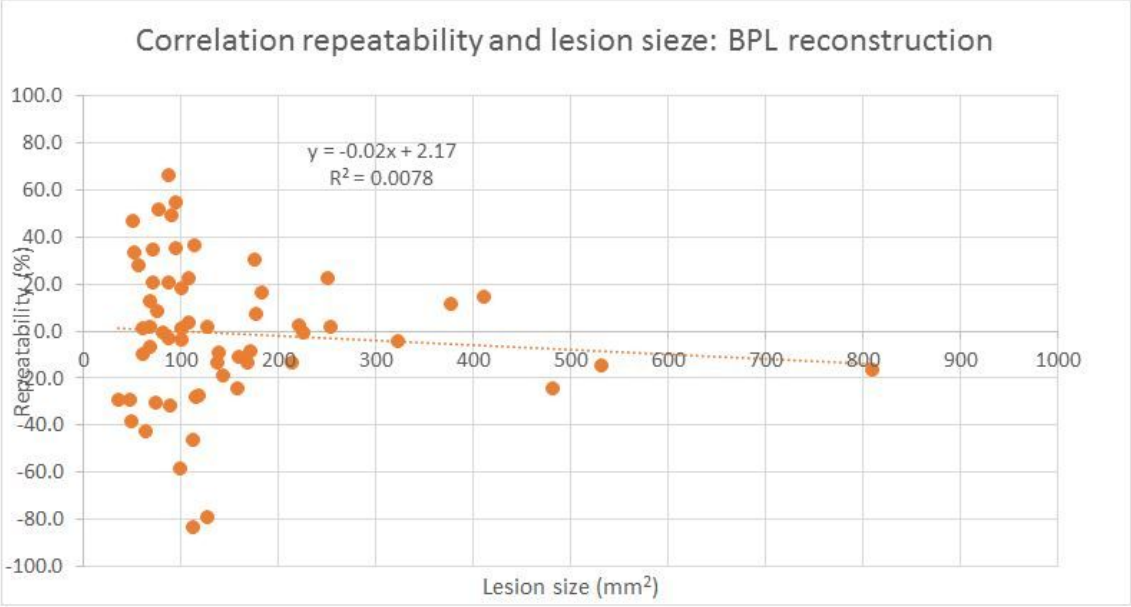

Figure 2

Correlation of repeatability and lesion size for standard reconstructions (2A) and BPL reconstructions (2B).